Retinotopic fMRI Reveals Visual Dysfunction and Functional Reorganization in the Visual Cortex of Mild to Moderate Glaucoma Patients

Wei Zhou, PhD, Eric R. Muir, PhD, Kundandeep S. Nagi, MD, Steven Chalfin, MD, Pavel Rodriguez, MD, and Timothy Q. Duong, PhD

Purpose: To investigate retinotopic functional representation in the visual cortex of mild to moderate primary open-angle glaucoma (POAG) participants and age-matched normal volunteers using high-resolution retinotopic blood oxygenation level dependent (BOLD) functional magnetic resonance imaging (fMRI).

Methods: fMRI was performed on 9 POAG participants (61 ± 11 y old) and 9 age-matched controls (58 ± 5 y old) were studied. A wide-view visual presentation (± 55 degrees) was used to evaluate central and peripheral vision. Cortical magnification factors and BOLD% changes as a function of eccentricity. Correlation analysis between BOLD% changes and visual field scores, and between BOLD% changes and retinal nerve fiber layer thicknesses was performed. Comparison of BOLD% changes for individual visual field quadrants between POAG subgroups and normal group was performed.

Results: BOLD% changes of POAG participants in peripheral visual regions were reduced compared to normals but similar in central visual regions, consistent with the notion of peripheral vision being affected first and more compared to central vision. fMRI retinotopic mapping revealed enlarged representation of the parafovea in the visual cortex of POAG participants compared to normals. Cortical magnification of the central, but not peripheral, visual representation in the visual cortex was larger in POAG participants, suggesting functional remapping. BOLD% changes of individual visual field quadrants were significantly correlated with visual field scores and with retinal nerve fiber layer thickness in the corresponding quadrants.

Conclusions: These results support the hypothesis that there are functional alteration and remapping in the topographic representation of the visual cortex in POAG participants, and these changes are correlated with disease severity.

Key Words: functional remodeling, functional remapping, retinotopic, primary open-angle glaucoma, visual cortex, visual field, functional magnetic resonance imaging, blood oxygenation level dependent (BOLD) fMRI

(*J Glaucoma* 2017;26:430–437)

Primary open-angle glaucoma (POAG), the most prevalent form of glaucoma, is a leading cause of blindness, affecting 3 million Americans.[1] POAG is characterized by progressive loss of retinal ganglion cells and optic nerve damage, resulting in loss of peripheral vision followed by loss of central vision.[2–5] Elevated intraocular pressure (IOP) is a known risk factor, and lowering IOP is the only available treatment for glaucoma.[6] However, many glaucoma patients continue to lose vision despite successful treatment to lower IOP.[7] As such, there are likely other factors that contribute to the disease pathogenesis and progression. It has been suggested that there is concurrent neurodegeneration and neuronal dysfunction in the brain visual pathway.

A number of anatomic MRI studies have found evidence of gray matter atrophy in the visual cortex of glaucoma patients[8–13] and diffusion-tensor MRI studies have found abnormal white matter in the optic nerve, optic chiasm, optic tract, and optic radiation.[14–19] Functional magnetic resonance imaging (fMRI) can be used to detect brain activation due to visual cues, however there are only a few fMRI studies of glaucoma patients and the results are controversial.[20–23] Three studies found blood oxygenation level dependent (BOLD) fMRI% changes to decrease with glaucoma severity in POAG participants,[20,21,23] whereas another study reported BOLD responses to increase with glaucoma severity.[22] These fMRI studies used simple retinotopic stimuli and low spatial resolution (> 3 mm), which limited functional parcellation of the retinotopic representation in the visual cortex. Comparisons of fMRI and clinical data were made with respect to the left and right eyes (not left and right visual fields), confounding interpretation because the visual pathways are segregated by visual field after the optic chiasm and thus the unilateral posterior visual pathway receives input from the ipsilateral retina and the contralateral visual field from both eyes. Importantly, previous fMRI studies of glaucoma used narrow-view visual stimuli (about ± 12 degrees of only the central visual field), precluding assessment of peripheral vision which is often affected in early glaucoma, whereas central vision is not affected until late stage glaucoma.[24] Thus, it remains unclear to what extent, if any, the central and peripheral visual function in the visual cortex is altered in glaucoma.

The goal of this study was to use high-resolution retinotopic fMRI with wide-field (± 55 degrees) stimuli to evaluate neuronal function in the visual cortex of POAG participants in comparison with age-matched normal controls. Two types of visual stimuli were assessed, expanding rings to evaluate brain activation patterns as a function of eccentricity and rotating wedges to evaluate activation per

Received for publication August 5, 2016; accepted January 11, 2017.
From the Department of Ophthalmology, Research Imaging Institute, University of Texas Health Science Center, San Antonio, TX.
W.Z., E.R.M., and T.Q.D. designed research and wrote the paper; W.Z., K.S.N., S.C., and P.R. performed research; W.Z. and E.R.M. analyzed data.
Disclosure: The authors declare no conflict of interest.
Reprints: Timothy Q. Duong, PhD, Department of Ophthalmology, University of Texas Health Science Center at San Antonio, 8403 Floyd Curl Dr, San Antonio, TX 78229 (e-mail: duongt@uthscsa.edu).

DOI: 10.1097/IJG.0000000000000641

visual field quadrant. BOLD fMRI% changes and cortical magnification were analyzed as a function of eccentricity to evaluate changes in brain function corresponding to central and peripheral vision and to assess whether cortical remapping occurs in glaucoma. BOLD fMRI% changes were also evaluated for each visual field quadrants and comparisons were made with the corresponding clinical visual field scores and retinal nerve fiber layer (RNFL) thickness in individual quadrants instead of individual eyes. Both fMRI and clinical data were analyzed as a function of eccentricity, tabulated for central and peripheral visual fields as well as 4 visual quadrants for comparison. The central hypothesis is that there are visual dysfunction and retinotopic and remapping in the visual cortex of POAG participants compared to age-matched normals.

METHODS

Participants

Nine participants diagnosed with POAG [36 to 74 (61 ± 11, mean ± SD) y old, 4 males] and 9 age-matched healthy volunteers [53 to 65 (58 ± 5) y old, 6 males] were enrolled. Participants gave written informed consent and were financially compensated for their time to participate in this study. This study was approved by the Institutional Review Board of the University of Texas Health Science Center at San Antonio.

The clinical diagnosis of POAG was performed or confirmed by 2 qualified ophthalmologists (S.C. and K.N.). The glaucoma diagnosis was made based on the diagnostic criteria of the American Academy of Ophthalmology's Glaucoma Primary Open-Angle Glaucoma Preferred Practice Pattern Guidelines[25] through assessment of the open anterior chamber angle, identification of visual field defects typical of glaucoma, optic disc cupping, or identification of an IOP of 21 mm Hg or greater. Severity of glaucoma was categorized as mild, moderate and severe based on established criteria.[25,26] Exclusion criteria were any retained metallic foreign body or implanted device, history of claustrophobia, neurological or psychiatric disorders, diabetes, eye surgery, other eye diseases (except myopia), and clinically abnormal structural brain MRI. Normal controls were age-matched participants free of all eye diseases with the same exclusion criteria (myopia was also not excluded). MRI-compatible goggles to provide refractive correction were used for 1 subject who otherwise could not see the stimuli clearly.

Clinical Measurements

For POAG patients, visual fields were acquired using 24-2 automated perimetry (HFA II 750, Carl Zeiss, Dublin, CA) to derive pattern SD (PSD). A mean binocular PSD was obtained by taking the mean PSD of the 2 eyes point by point, then averaged for each of the 4 quadrants. Glaucoma severity was graded for each quadrant as[26]: early defect: PSD > −6.00 dB; moderate defect: PSD of −6.01 dB to −12.00 dB; advanced defect: PSD of −12.01 dB to −20.00 dB; severe defect: PSD < −20.00 dB. One participant was diagnosed with advanced defect in at least 1 quadrant, and no POAG participants were diagnosed with any severe defects.

RNFL thickness was obtained using optical coherence tomography (Spectralis Tracking Laser Tomography, Heidelberg Engineering, Heidelberg, Germany). Thus, the mean RNFL thickness for each quadrant was obtained by taking the weighted average of RNFL thicknesses from clinical optical coherence tomography data for each eye, and then averaged for the 2 eyes for the corresponding quadrant.

IOP was also measured using Goldmann applanation tonometry (Haag-Streit Diagnostics, Bern, Switzerland).

Visual Stimulation

For fMRI studies, a custom-made, wide-view visual presentation system was used to achieve a large visual field of ± 55 × ± 55 degrees (horizontal × vertical), whereas typical visual stimulation fMRI studies use < ± 15 × ± 15 degrees. A screen (15 × 15 cm) on which stimuli were projected was placed 10 cm from the participant's eyes. During the MRI studies, participants were asked to fixate on a white cross (3 × 3 degrees) on a gray background at the center of the stimuli. Two separate visual stimulation paradigms were presented: a series of rotating wedges and a series of expanding or contracting rings. For the wedge stimuli, 12 frames of clockwise or counterclockwise rotating wedges, extending to 110 degrees visual field of view (FOV), with 8 Hz contrast-reversing checkerboard pattern (100% contrast) were displayed with a period of 30 seconds (an angular velocity over of 6 degrees/s) and were cycled 6 times. For the ring stimuli, 8 frames of expanding or contracting rings, covering 110 degrees visual FOV, with 8 Hz contrast-reversing checkerboard pattern (100% contrast) were displayed with a period of 30 seconds (with a speed for expanding or contracting of 1.8 degrees/s) and were cycled 6 times. The white cross was shown 10 seconds at the beginning and 10 seconds at the end of the each paradigm for obtaining baseline BOLD data. Each fMRI trial thus lasted 200 seconds.

MRI Acquisition

MRI data were collected on a 3 T scanner (Magnetom Trio, Siemens, Erlangen, Germany) with an 8-channel head coil. For each participant, anatomic MRI was acquired with a T1-weighted MP-RAGE sequence with repetition time (TR) of 2.2 seconds, echo time (TE) of 2.8 ms, FOV of 176 × 256 × 208 mm, spatial resolution of 1 × 1 × 1 mm, bandwidth of 190 Hz/pixel, flip angle of 13 degrees, and scan duration of 3 minutes 8 seconds. BOLD fMRI was acquired using the posterior half of the 8-channel head coil to provide a larger viewing angle unobstructed by the anterior half of the coil. A gradient-echo, echo-planar imaging sequence was used with TR of 2 seconds, TE of 30 ms, FOV of 220 × 220 mm, in-plane resolution of 1.7 × 1.7 mm, 29 of slices with thickness of 3 mm, and bandwidth of 1500 Hz/pixel. Each fMRI trial lasted 200 seconds. The fMRI slices were acquired parallel to the calcarine fissure.

Image Analysis

Image Preprocessing

The T1-weighted 3-dimensional MRI anatomic image was processed in Freesurfer (version 5.3.0, https://surfer.nmr.mgh.harvard.edu/fswiki/recon-all) for cortical surface reconstruction as a reference for each participant. The occipital cortex of each brain was then virtually cut along the calcarine fissure and then flattened onto surfaces. Raw fMRI data were screened and corrected as needed using AFNI (https://afni.nimh.nih.gov/pub./pub/dist/doc/program_help/3dvolreg.html). fMRI images were coregistered onto the reconstructed cortical surface and then smoothed by a 5-mm kernel in Freesurfer.

Phase-encoded Processing

Phase-encoded retinotopic maps were obtained by correlating the BOLD fMRI time series with a modeled response function of the stimulus paradigm.[27] Canonical hemodynamic delay was applied to construct the response function. A significance level of $P < 0.01$ was applied to the phase correlation maps. The activation maps were color-coded and overlaid on the virtually flattened visual cortex. The boundaries of the retinotopic areas (V1, V2, and V3) were defined for each participant by field sign maps from the wedge stimuli.[28]

Cortical Magnification Measurement

From the ring stimuli, the cortical distances of activation clusters relative to the center of the dorsal and ventral activation patterns were calculated for different eccentricities through Dijkstra's algorithms in Freesurfer. These data were used to calculate the linear cortical magnification factor M as the ratio of cortical distance d (in mm) and eccentricity θ (in degrees). M was calculated separately in V1, V2, and V3 using the boundaries of the retinotopic areas from the phase maps of the wedge stimuli.

BOLD% Change Calculation

Statistical BOLD fMRI maps were calculated for both wedge and ring stimuli using general linear model in FSL (FMRIB Software Library, version 5.0, http://fsl.fmrib.ox.ac.uk/fsl) with a z-score threshold ≥ 2.3. For analysis by quadrant, the 12 wedge stimuli were grouped by the 4 visual field quadrants (3 frames per quadrant) to define the general linear model in FSL. The activation maps were then overlaid on the virtually flattened cortical surface. A region of interest (ROI) for each quadrant was manually drawn to include all the activated voxels with a z-score above 2.3. The average fMRI% changes were tabulated for individual quadrants and were analyzed as a function of glaucoma severity for the individual quadrants. fMRI data by visual field quadrants were correlated with visual field function and RNFL thickness for the corresponding quadrants.

The ring stimuli were grouped by eccentricity for each of the 8 frames, and ROIs for different eccentricities were manually drawn based on the activated voxels (with a z-score >2.3) regions for each frame. BOLD% changes were then calculated and plotted as a function of eccentricity. Eccentricity data were also binned into central ($< \pm 12$ degrees) and peripheral ($> \pm 12$ degrees) regions, where $\pm$ 12-degree visual stimulus presentation is typically used for visual fields and in prior retinotopic fMRI studies.[20–23]

Statistics

Comparison of age between normals and glaucoma participants used 2-sample t test. Comparison of the cortical magnification factors and BOLD% changes as a function of eccentricity between normal and POAG participants used a mixed-effect 2-factor analysis of variance (ANOVA) with group and eccentricity as fixed factors and subject as a random effect factor. For the cortical magnification, 3 separate ANOVAs were run for data from V1, V2, and V3. Averaged BOLD% change in both central ($< \pm 12$ degrees of the visual field) and peripheral ($> \pm 12$ degrees of the visual field) regions were compared between groups using 1-way ANOVA with P-values adjusted by Bonferroni post hoc correction. Correlation analysis between BOLD% changes and visual field scores, and between BOLD% changes and RNFL thicknesses used Spearman's correlation. Comparison of BOLD% changes for individual quadrants between POAG subgroups and normal group used a mixed-effect 1-factor ANOVA with group/subgroup as the fixed factor and quadrant and subject as random effect factors with Tukey post hoc correction. $P < 0.05$ was considered to be significantly different unless otherwise specified.

RESULTS

Clinical data of POAG participants are shown in Table 1. There were no significant age differences between normal and glaucoma participants ($P > 0.05$, t test). Visual field scores, as measured by PSD, of all POAG participants were abnormal compared to age-corrected normative database. All participants were under standard medical care for glaucoma to maintain IOPs within normal physiological ranges (< 21 mm Hg), except 1 newly diagnosed participant (#5) who still had elevated IOP. RNFL thicknesses of the majority of POAG participants were abnormal compared to age-corrected normative database.

The retinotopic fMRI polar (wedge stimuli) and eccentricity (ring stimuli) maps from a normal and a POAG participant are shown in Figure 1. Polar maps showed

TABLE 1. Clinical Characteristics of Individual POAG Subjects

	Visual Field (dB)					
	OD	OS	IOP (mm Hg)		RNFL (μm)	
No	PSD	PSD	OD	OS	OD	OS
1	−1.94	−3.31	14	15	77*	66**
2	−2.32	−1.3	15	16	104	113
3	−1.6	−4.75	12	18	88	76*
4	−12.92	−9.58	14	16	44**	69**
5	−1.3	−3.2	31	51	80*	67**
6	−7.49	−2.54	10	10	73**	92
7	−10.43	−7.97	17	16	71**	78*
8	−3.03	−2.76	14	15	87	88
9	−1.94	−1.67	19	19	78*	97

Visual field data, IOP, and RNFL are shown for left (oculus sinister) and right (oculus dexter) eyes.
*$P < 0.05$.
**$P < 0.01$ indicates RNFL thickness of inner cycle significantly different from built-in normative data set.
IOP indicates intraocular pressure; POAG, primary open-angle glaucoma; PSD, pattern SD; RNFL, retinal nerve fiber layer thickness.

Copyright © 2017 Wolters Kluwer Health, Inc. All rights reserved.

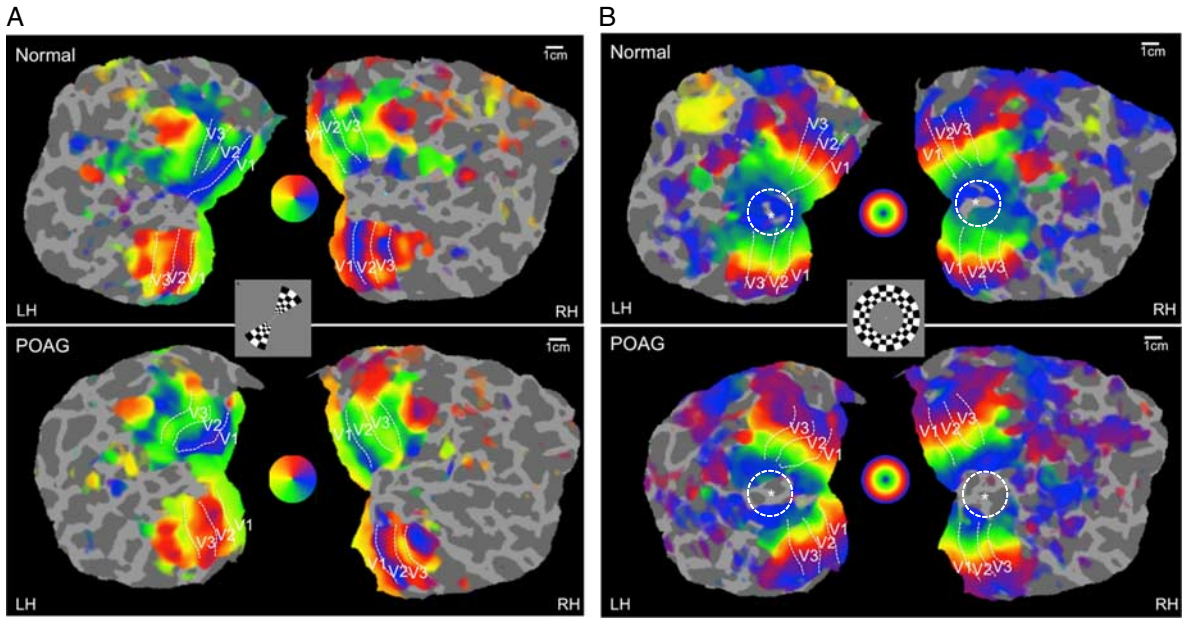

FIGURE 1. (A) Polar and (B) eccentricity maps of left and right hemispheres (LH and RH) from a normal participant and a primary open-angle glaucoma (POAG) participant. The boundaries of V1, V2, and V3 cortical regions are also delineated. The inset in the center shows a static representation of the rotating wedge and expanding ring stimuli (contrast-reversing checkerboard at 8 Hz and 100% contrast). Figure 1 can be viewed in color online at www.glaucomajournal.com.

expected activation patterns with no apparent differences between normal and POAG participants. Eccentricity maps showed the centermost foveal region to be largely void of activation in both groups as expected because the static fixation cross evoked no BOLD% changes. However, the activated area of the parafovea (blue pixels) appeared larger in POAG participants compared to normals, suggesting functional remapping in the visual cortex.

To quantify the observed central visual differences between groups, the cortical magnification factor (M) was analyzed as a function of eccentricity (Fig. 2). M decreased with increasing eccentricity in V1, V2, and V3 for both normal and POAG participants, as expected. However, M was larger in POAG participants at smaller eccentricities compared to normals. M was significantly different between POAG participants and normals in V1 (mixed-effect ANOVA with Tukey post hoc correction, Group factor: $F = 17.57$, $P < 0.0001$; interaction: $F = 3.76$, $P < 0.001$), and V2 (Group factor: $F = 12.79$, $P < 0.001$; interaction: $F = 3.83$, $P < 0.001$), but not in V3 (Group factor: $F = 3.34$, $P > 0.05$, interaction: $F = 1.60$, $P > 0.05$).

To further investigate the altered cortical representation between normal and POAG participants, BOLD% changes were analyzed as a function of eccentricity (Fig. 3A) and binned into central ($< \pm 12$ degrees) and peripheral ($> \pm 12$ degrees) visual field (Fig. 3B). The overall eccentricity profile of the POAG group showed significant reduction compared with normal participants (mixed-effect ANOVA, Group factor: $F = 28.68$, $P < 10^{-6}$; interaction: $F = 1.61$, $P > 0.05$). At smaller eccentricity, BOLD% changes were slightly but not significantly reduced between POAG participants and normal

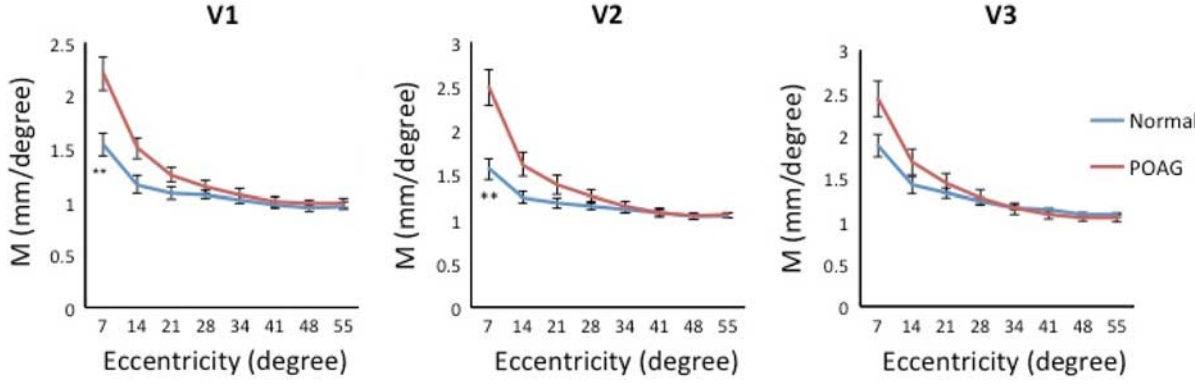

FIGURE 2. Average cortical magnification factor (M) as a function of eccentricity of V1, V2, and V3 from normal and primary open-angle glaucoma (POAG) participants. Mean ± SEM. M was significantly different between POAG participants and normals in V1 ($F = 17.57$, $P < 0.0001$, 2-factor ANOVA with post hoc correction), and V2 ($F = 12.79$, $P < 0.001$), but not in V3 ($F = 3.34$, $P > 0.05$). Figure 2 can be viewed in color online at www.glaucomajournal.com.

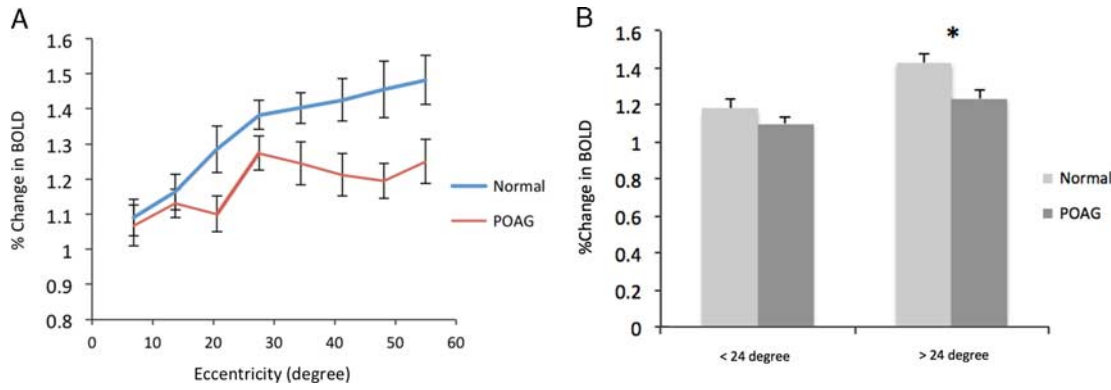

FIGURE 3. Averaged BOLD% change from normal and POAG participants (A) as a function of eccentricity and (B) binned for $< \pm 12$ and $> \pm 12$ degrees visual field. Mean ± SEM. $^*P < 0.05$, 2-factor ANOVA with post hoc correction. Figure 3 can be viewed in color online at www.glaucomajournal.com.

participants. At larger eccentricity, BOLD% changes were significantly reduced in POAG participants compared to normal participants ($P < 0.05$, 1-way ANOVA with Bonferroni post hoc).

The PSD map of a representative visual field test of the right and left eyes from a POAG participant are shown in Figure 4A. Abnormal PSD relative to a normative database are apparent in the upper visual field. The mean binocular PSD were obtained by averaging the 2 eyes for the corresponding visual field quadrants. The BOLD% changes, tabulated for individual quadrants, were significantly correlated with mean PSD by quadrants ($\rho = 0.48$, $P < 0.005$) (Fig. 4B). When binned by glaucoma severity (Fig. 4C), BOLD% changes of advanced ($0.44\% \pm 0.05\%$, $P < 0.05$, mixed-effect ANOVA with Tukey post hoc for multiple comparison) and moderate POAG participants ($0.65\% \pm 0.10\%$, $P < 0.01$) were significantly different from normal participants ($1.02\% \pm 0.05\%$), whereas the BOLD% changes of early POAG participants ($0.97\% \pm 0.07\%$) only showed a trend but not statistically significantly different from normal participants ($P > 0.05$).

Representative RNFL thickness data from the right and left eyes of a POAG participant are shown in Figure 5A. The mean RNFL thickness for each quadrant was obtained by taking the weighted average of RNFL thicknesses for each eye, followed by averaging the 2 eyes for the corresponding visual field quadrants. BOLD% changes by quadrants were significantly correlated with the mean RNFL thickness of the corresponding quadrants ($\rho = 0.447$, $P < 0.01$; Fig. 5B).

DISCUSSION

This study investigated the retinotopic representation in the visual cortex of POAG participants using wide-view visual presentation, high-resolution retinotopic stimuli, and high-resolution BOLD fMRI. BOLD fMRI data were analyzed as a function of eccentricity. BOLD fMRI data were correlated with visual field function and RNFL thickness of the corresponding visual field quadrants. The major findings are: (i) retinotopic fMRI shows enlarged activation of the central visual representation in POAG compared to normal participants, suggesting remapping of the parafoveal cortical regions in glaucoma, (ii) cortical magnification of the central, but not peripheral, visual field in the visual cortex is larger in POAG participants compared to normals, corroborating the notional of functional remapping, (iii) BOLD% changes of POAG participants are reduced at larger eccentricity (peripheral visual field) compared to normals but are similar at small eccentricity (central visual field), consistent with the notion that

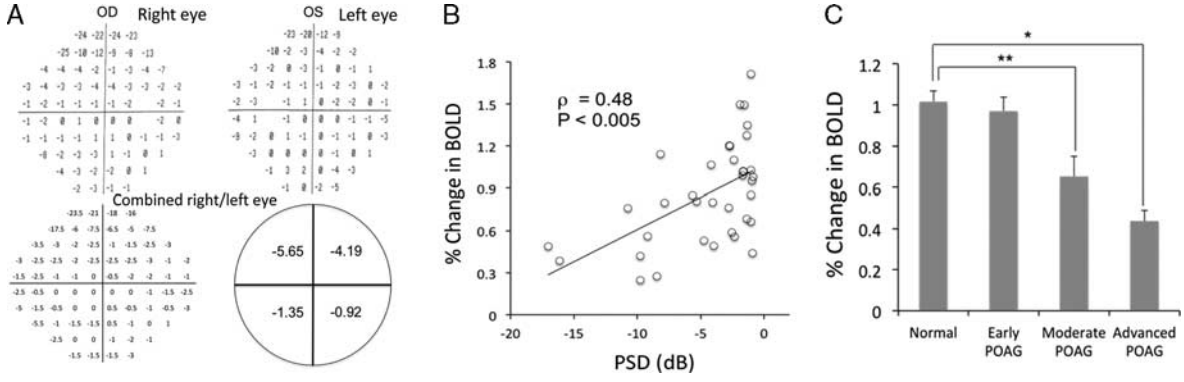

FIGURE 4. A, Pattern SD (PSD) scores of each eye and the combined (mean) PSD of the 2 eyes calculated by taking the mean point by point. B, Correlation of BOLD% changes from individual quadrants with visual field score PSD. Each data point is from an individual quadrant and some points overlapped. C, Average BOLD signal changes from individual quadrants among normal and POAG subgroups. Mean ± SEM. $^*P < 0.05$, $^{**}P < 0.01$ using a 2-factor ANOVA. OD indicates oculus dexter; OS, oculus sinister.

Copyright © 2017 Wolters Kluwer Health, Inc. All rights reserved.

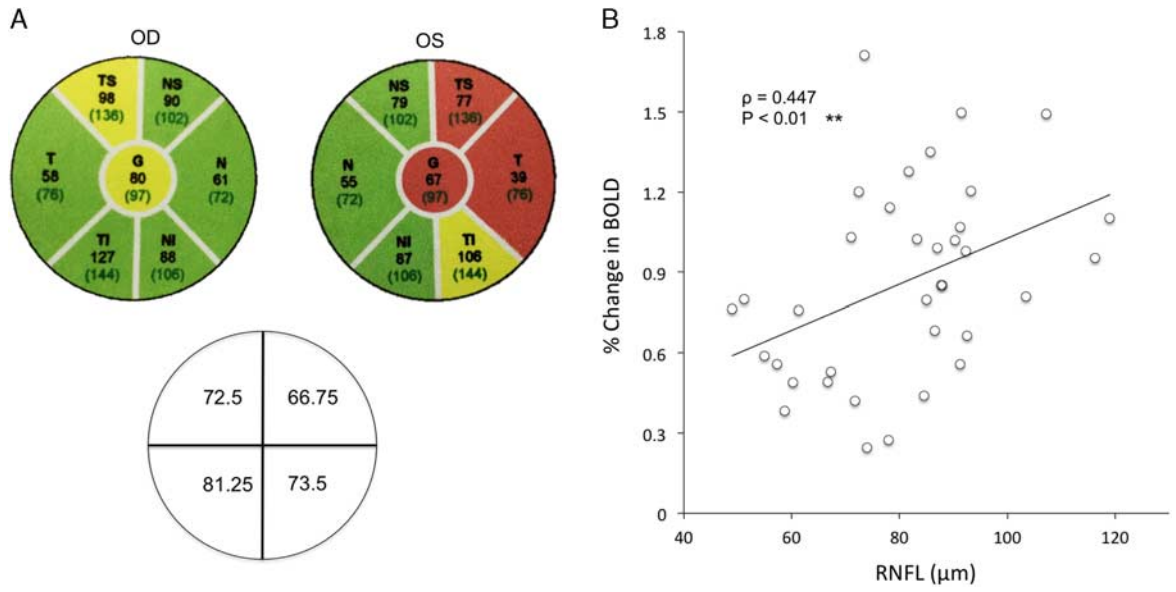

FIGURE 5. A, Retinal nerve fiber layer (RNFL) thicknesses of each eye and the combined (mean) RNFL thickness per quadrant of the 2 eyes calculated by taking weighted average. B, Correlation of BOLD% changes from individual quadrants with RNFL thickness. Each data point is from an individual quadrant. $^{**}P<0.01$. OD indicates oculus dexter; OS, oculus sinister. Figure 5 can be viewed in color online at www.glaucomajournal.com.

glaucoma affects peripheral vision first, and (iv) fMRI BOLD% changes of visual field quadrants are significantly correlated with visual field function and RNFL thickness in the corresponding quadrants in POAG participants. These results support the hypothesis that there are functional alterations and remapping of retinotopic representation in the visual cortex in patients with open-angle glaucoma, and these changes are correlated with disease severity.

Retinotopic Remapping in the Visual Cortex

The activated areas of the parafovea appeared enlarged in POAG participants compared to normals, suggesting functional remapping in the visual cortex. This observation was corroborated by data on cortical magnification factors, which were larger in POAG participants compared to normals at small but not large eccentricity. Several studies have reported adult cortical adaptation or remapping in ocular disorders but none in glaucoma to our knowledge. For example, patients with amblyopia exhibited cortical alterations in receptive field size and responsiveness.[29–31] Patients with macular degeneration showed functional remapping with increased neural activation in the lesion projected zones of visual cortex, suggesting recruitment of unused brain tissue for other similar functions,[32,33] although it remains controversial.[33,34] Our results suggest that the visual cortex of the POAG participants was remodeled to take over the reduced peripheral visual fields, resulting in an enlarged cortical magnification factors at low eccentricity in POAG compared to control participants. The changes as a function of eccentricity were spatially continuous and orderly. Glaucoma is a progressive disease and the slow loss of visual function perhaps enables remapping to take place in such an orderly fashion.

Decreased BOLD Responses in POAG

The BOLD responses in the visual cortex were reduced in POAG compared to normal participants. A few studies have previously reported overall attenuated visual-evoked fMRI responses in the visual cortex in glaucoma participants compared with the normal appearing fellow eye[20,22] and with normal participants.[23] Although our results are in general agreement with these prior fMRI studies, we further showed for the first time that the extent of attenuated BOLD responses in the visual cortex is dependent on eccentricity, with BOLD% changes at larger eccentricity being attenuated more than at lower eccentricity in mild to moderate POAG participants. This observation is consistent with the notion of peripheral vision being affected first and more extensively compared to central vision in glaucoma.[24,35] A likely explanation for the reduced BOLD fMRI responses is that there is reduced neural input to the visual cortex as a result of degeneration of retinal ganglion cells,[24] magnocellular layers of the lateral geniculate nucleus,[36] and axons in the optic nerve, optic tract and optic radiation[15,17,18] due to glaucoma. The reduced BOLD% changes in the periphery are likely associated with the enlarged central visual representation.

BOLD Responses Versus Clinical Measures

BOLD% changes in individual visual quadrants were significantly correlated with visual field function in the corresponding quadrants. The literature on this is sparse and controversial. Duncan et al[20,21] found the average fMRI responses of the entire visual cortex to be correlated with visual field scores by individual eyes instead of visual field quadrants, in general agreement with our results. Using ROIs from an anatomic atlas, Gerente et al[23] found that visual fields had a significant association with corresponding BOLD% changes per quadrant in glaucoma and controls but the group fMRI data showed no differences between glaucoma and control participants. Qing et al[22] surprisingly found that the BOLD% changes increased with decreased visual field function difference when comparing normal with fellow glaucomatous eyes,

and they interpreted the increased BOLD% changes as overcompensation from brain replasticity.

The narrow-view stimuli in the prior studies likely contributed to the inconsistency. There is evidence that peripheral vision is affected first and central vision is usually not affected until late-stage glaucoma.[24,35,37,38] Indeed, we found the largest differences in BOLD% changes at large eccentricity, providing the first BOLD fMRI evidence that peripheral vision is affected first before central vision. We also correlated BOLD% changes with visual field quadrants (instead of with individual eyes[20,21]), an appropriate comparison because the visual field information of each eye separates at the optic chiasm and projects onto the visual cortex. Comparison with respect to each eye, instead of visual field, could lead to incorrect delineation of visual dysfunction if glaucoma defect is asymmetric with respect to the 2 eyes or visual field quadrants. Another potential explanation is that we prescribed our ROI based on functional retinotopic map instead of anatomic atlas as in.[23] It is also possible that we used comparatively high-resolution BOLD fMRI. Further investigation is needed to fully address these apparent discrepancies.

BOLD% changes in individual visual quadrants were also significantly correlated with RNFL thickness in POAG participants. BOLD% changes have been found to correlate[20,23] and not correlate[22] with RNFL thicknesses. Structure (RNFL thinning) and function (vision loss) could be affected differently at different stage of glaucoma. For example, RNFL has been found to continue to reduce in thickness while visual field function remains normal until late stage[39] because there is functional compensation.[40] Visual field defects are detected only after a substantial number of retinal ganglion cells have already died.[2–5]

Limitations and Future Directions

There are several limitations of this study. (1) The number of participants, although typical for similar fMRI studies, was relatively small and only mild to moderate POAG participants were studied. Although it is intriguing that these changes were detectable in mild to moderate POAG participants, inclusion of severe POAG participants would be helpful to further corroborate functional remapping in the visual cortex. (2) Although our spatial resolution is high compared to most previous fMRI studies in glaucoma, further increase in spatial resolution would help to improve parcellation of the retinotopic representation, including finer parcellation beyond 4 visual field quadrants. (3) Structural atrophy of the visual cortex in glaucoma[12] could potentially affect the calculation of cortical magnification factor. Although our data showed that there were fMRI changes in the visual cortex in the fovea/parafovea, the calculation of M could be inaccurate because the observed cortical remapping affected the calculation of M per se. It is perhaps more accurate to state that cortical remapping affects the estimates of M, giving the appearance that M is greater at the fovea. Clinical visual field scores used monocular stimuli, whereas fMRI used binocular stimuli. Using the same type (either monocular or binocular) of stimulus presentation would simplify comparison, as combining by taking the mean may not be an ideal method. In addition, acquisition of visual fields covering different visual angles would be useful in future studies, as we found reduced BOLD response at eccentricities larger than those tested by perimetry herein as well as increased cortical magnification at low eccentricities for which it would help to have denser sampling of central visual fields. It would be of interest to use wide-field retinotopic fMRI to investigate the onset and progression of abnormal BOLD fMRI response as a function of eccentricity relative to those of abnormal clinical parameters (ie, visual field score and RNFL). It is also of interest to employ fMRI to study moving stimuli as loss of motion perception has been reported in glaucoma.[41]

CONCLUSIONS

This study investigated retinotopic visual function in the visual cortex of POAG participants using wide-view visual stimuli to investigate function in the visual cortex from central to peripheral vision. fMRI findings were correlated with the corresponding visual field function and RNFL thickness in individual visual field quadrants. Our results support the hypothesis that there is altered visual function and retinotopic remapping in the visual cortex of mild and moderate POAG participants, further supporting the notion that neural dysfunction is involved in the glaucoma pathogenesis and progression. Retinotopic fMRI has the potential to improve staging of glaucoma progression and helps to improve understanding of the pathogenesis of the disease.

ACKNOWLEDGMENTS

The authors thank Jinqi Li, Betty Heyl, and Daniel Mojica for assistance with IRB protocol and participant recruitment. This work was funded in part by NIH/NEI (R01- EY021179), S.I. Glickman Endowment for Ophthalmic Research, Amor B. and Loddie Lee Whitehead Fellowship Fund in Ophthalmic Research.

REFERENCES

1. Kapetanakis VV, Chan MP, Foster PJ, et al. Global variations and time trends in the prevalence of primary open angle glaucoma (POAG): a systematic review and meta-analysis. *Br J Ophthalmol*. 2016;100:86–93.
2. Kerrigan-Baumrind LA, Quigley HA, Pease ME, et al. Number of ganglion cells in glaucoma eyes compared with threshold visual field tests in the same persons. *Invest Ophthalmol Vis Sci*. 2000;41:741–748.
3. Quigley HA, Addicks EM, Green WR. Optic nerve damage in human glaucoma. III. Quantitative correlation of nerve fiber loss and visual field defect in glaucoma, ischemic neuropathy, papilledema, and toxic neuropathy. *Arch Ophthalmol*. 1982;100:135–146.
4. Smith EL 3rd, Hung LF, Harwerth RS. Developmental visual system anomalies and the limits of emmetropization. *Ophthalmic Physiol Opt*. 1999;19:90–102.
5. Limb GA, Martin KR. Res S. A. P. O.. Current prospects in optic nerve protection and regeneration: sixth ARVO/Pfizer Ophthalmics Research Institute Conference. *Invest Ophth Vis Sci*. 2011;52:5941–5954.
6. AGIS. The Advanced Glaucoma Intervention Study (AGIS): 7. The relationship between control of intraocular pressure and visual field deterioration.The AGIS Investigators. *Am J Ophthalmol*. 2000;130:429–440.
7. Coleman AL, Miglior S. Risk factors for glaucoma onset and progression. *Surv Ophthalmol*. 2008;53(suppl 1):S3–S10.
8. Lee JY, Jeong HJ, Lee JH, et al. An investigation of lateral geniculate nucleus volume in patients with primary open-angle glaucoma using 7 tesla magnetic resonance imaging. *Invest Ophthalmol Vis Sci*. 2014;55:3468–3476.

9. Gupta N, Greenberg G, de Tilly LN, et al. Atrophy of the lateral geniculate nucleus in human glaucoma detected by magnetic resonance imaging. *Br J Ophthalmol*. 2009;93:56–60.
10. Zikou AK, Kitsos G, Tzarouchi LC, et al. Voxel-based morphometry and diffusion tensor imaging of the optic pathway in primary open-angle glaucoma: a preliminary study. *AJNR Am J Neuroradiol*. 2012;33:128–134.
11. Chen WW, Wang N, Cai S, et al. Structural brain abnormalities in patients with primary open-angle glaucoma: a study with 3T MR imaging. *Invest Ophthalmol Vis Sci*. 2013;54:545–554.
12. Yu L, Xie B, Yin X, et al. Reduced cortical thickness in primary open-angle glaucoma and its relationship to the retinal nerve fiber layer thickness. *PLoS One*. 2013;8:e73208.
13. Yu L, Yin X, Dai C, et al. Morphologic changes in the anterior and posterior subregions of V1 and V2 and the V5/MT + in patients with primary open-angle glaucoma. *Brain Res*. 2014;1588:135–143.
14. Hernowo AT, Boucard CC, Jansonius NM, et al. Automated morphometry of the visual pathway in primary open-angle glaucoma. *Invest Ophthalmol Vis Sci*. 2011;52:2758–2766.
15. Dai H, Yin D, Hu C, et al. Whole-brain voxel-based analysis of diffusion tensor MRI parameters in patients with primary open angle glaucoma and correlation with clinical glaucoma stage. *Neuroradiology*. 2013;55:233–243.
16. Michelson G, Engelhorn T, Warntges S, et al. DTI parameters of axonal integrity and demyelination of the optic radiation correlate with glaucoma indices. *Graefes Arch Clin Exp Ophthalmol*. 2013;251:243–253.
17. Garaci FG, Bolacchi F, Cerulli A, et al. Optic nerve and optic radiation neurodegeneration in patients with glaucoma: in vivo analysis with 3-T diffusion-tensor MR imaging. *Radiology*. 2009;252:496–501.
18. El-Rafei A, Engelhorn T, Warntges S, et al. Glaucoma classification based on visual pathway analysis using diffusion tensor imaging. *Magn Reson Imaging*. 2013;31:1081–1091.
19. Chang ST, Xu J, Trinkaus K, et al. Optic nerve diffusion tensor imaging parameters and their correlation with optic disc topography and disease severity in adult glaucoma patients and controls. *J Glaucoma*. 2014;23:513–520.
20. Duncan RO, Sample PA, Weinreb RN, et al. Retinotopic organization of primary visual cortex in glaucoma: a method for comparing cortical function with damage to the optic disk. *Invest Ophthalmol Vis Sci*. 2007;48:733–744.
21. Duncan RO, Sample PA, Weinreb RN, et al. Retinotopic organization of primary visual cortex in glaucoma: Comparing fMRI measurements of cortical function with visual field loss. *Prog Retin Eye Res*. 2007;26:38–56.
22. Qing G, Zhang S, Wang B, et al. Functional MRI signal changes in primary visual cortex corresponding to the central normal visual field of patients with primary open-angle glaucoma. *Invest Ophthalmol Vis Sci*. 2010;51:4627–4634.
23. Gerente VM, Schor RR, Chaim KT, et al. Evaluation of glaucomatous damage via functional magnetic resonance imaging, and correlations thereof with anatomical and psychophysical ocular findings. *PLoS One*. 2015;10:e0126362.
24. Glovinsky Y, Quigley HA, Dunkelberger GR. Retinal ganglion cell loss is size dependent in experimental glaucoma. *Invest Ophthalmol Vis Sci*. 1991;32:484–491.
25. Prum BE, Rosenberg LF, Gedde SJ, et al. Primary open-angle glaucoma preferred practice pattern® guidelines. *Ophthalmol*. 2016;123:P41–P111.
26. Mills RP, Budenz DL, Lee PP, et al. Categorizing the stage of glaucoma from pre-diagnosis to end-stage disease. *Am J Ophthalmol*. 2006;141:24–30.
27. Pitzalis S, Galletti C, Huang RS, et al. Wide-field retinotopy defines human cortical visual area v6. *J Neurosci*. 2006;26:7962–7973.
28. Sereno MI, Dale AM, Reppas JB, et al. Borders of multiple visual areas in humans revealed by functional magnetic resonance imaging. *Science*. 1995;268:889–893.
29. Conner IP, Odom JV, Schwartz TL, et al. Retinotopic maps and foveal suppression in the visual cortex of amblyopic adults. *J Physiol*. 2007;583:159–173.
30. Hussain Z, Svensson CM, Besle J, et al. Estimation of cortical magnification from positional error in normally sighted and amblyopic subjects. *J Vis*. 2015;15:25.
31. Kiorpes L, Kiper DC, O'Keefe LP, et al. Neuronal correlates of amblyopia in the visual cortex of macaque monkeys with experimental strabismus and anisometropia. *J Neurosci*. 1998;18:6411–6424.
32. Baker CI, Peli E, Knouf N, et al. Reorganization of visual processing in macular degeneration. *J Neurosci*. 2005;25:614–618.
33. Liu T, Cheung SH, Schuchard RA, et al. Incomplete cortical reorganization in macular degeneration. *Invest Ophthalmol Vis Sci*. 2010;51:6826–6834.
34. Baseler HA, Gouws A, Haak KV, et al. Large-scale remapping of visual cortex is absent in adult humans with macular degeneration. *Nat Neurosci*. 2011;14:649–U148.
35. Laquis S, Chaudhary P, Sharma SC. The patterns of retinal ganglion cell death in hypertensive eyes. *Brain Res*. 1998;784:100–104.
36. Yucel YH, Zhang Q, Gupta N, et al. Loss of neurons in magnocellular and parvocellular layers of the lateral geniculate nucleus in glaucoma. *Arch Ophthalmol*. 2000;118:378–384.
37. Nelson P, Aspinall P, O'Brien C. Patients' perception of visual impairment in glaucoma: a pilot study. *Br J Ophthalmol*. 1999;83:546–552.
38. McKean-Cowdin R, Varma R, Wu J, et al. Los Angeles Latino Eye Study, G. Severity of visual field loss and health-related quality of life. *Am J Ophthalmol*. 2007;143:1013–1023.
39. Bowd C, Zangwill LM, Berry CC, et al. Detecting early glaucoma by assessment of retinal nerve fiber layer thickness and visual function. *Invest Ophthalmol Vis Sci*. 2001;42:1993–2003.
40. Sharma SC. Changes of central visual receptive fields in experimental glaucoma. *Prog Brain Res*. 2008;173:479–491.
41. Silverman SE, Trick GL, Hart WM Jr. Motion perception is abnormal in primary open-angle glaucoma and ocular hypertension. *Invest Ophthalmol Vis Sci*. 1990;31:722–729.